

REVIEW ARTICLE OPEN



Skin-interfaced colorimetric microfluidic devices for on-demand sweat analysis

Weiye Liu¹, Huanyu Cheng²✉ and Xiufeng Wang¹✉

As sweat biomarker levels are continuously changing over metabolism and daily activities, pathological and physiological processes can be dynamically analyzed by wearable devices. The colorimetric skin-interfaced microfluidic devices that do not have external circuit modules exhibit enhanced deformability with a small footprint. However, it is difficult to achieve sampling over time and self-feedback for closed-loop systems. This review summarizes recent advances in microfluidic valves for biofluid management and chrono-sampling, as well as active triggers in microfluidics self-feedback. After enumerating the current limitations in temporal resolution and reliability, we further point out a few potential feasible strategies for future developments.

npj Flexible Electronics (2023)7:43; <https://doi.org/10.1038/s41528-023-00275-y>

INTRODUCTION

The increasing demand for preventive health/fitness monitoring has led to rapid developments of wearable devices that can detect biophysical and biochemical signals over various activities^{1–12}. Different from invasive/inconvenient blood sampling and intermittent sampling from urine, saliva¹³, tear¹⁴, or interstitial fluid^{15,16}, continuous in situ sweat analysis can be performed on most of the body surface due to sweat generation by human thermoregulation^{9,17} or local chemical stimulation¹⁸. Meanwhile, a large number of biomarkers in sweat have been correlated with the concentrations of circulating analyte in blood. Continuously monitoring changes in the concentration of these sweat biomarkers provides opportunities for early diagnosis of many diseases¹⁹, including cystic fibrosis, diabetes, and gout based on monitoring of chloride^{20,21}, glucose^{22,23}, uric acid and tyrosine²⁴. In addition, tracking sweat loss would provide personalized and time-sensitive feedback to athletes, military personnel, and physicians in clinical care for in-time water intake, which can prevent dehydration or heat stroke^{25–27}.

It is vital to collect, capture, and subsequently analyze (discrete) sweat samples at well-defined time points across body positions, leading to the efforts in the development of both electrochemical and colorimetric sweat sensors^{5,28}. With the bio-sensitive substances (e.g., enzymes, non-enzymatic nanomaterials, aptamers, molecularly imprinted polymers) decorated on the working electrode, the electrochemical biosensor can capture the target analyte and generate an electrical signal that correlates with the concentration. The sensor can either analyze the sweat with onboard electronics on skin²⁹ or collect sweat with a microfluidic network for subsequent analysis^{30,31}. With the circuit module³², the detection results can be transmitted to and displayed on terminal devices such as computers and mobile phones for visualization³³. Both enzymatic and nonenzymatic electrochemical biosensors are widely explored³⁴, with the former involving the use of enzymes and the latter using non-enzymatic nanomaterials. The enzymatic sensors often showcase high selectivity (e.g., enzymatic glucose sensor using glucose oxidase^{29,35}), but they are expensive, less stable over time, and are affected by environmental conditions^{36–38}. In contrast, nonenzymatic sensors can

exhibit high sensitivity, relatively good selectivity, and high stability^{30,39}. But they often show slow reaction kinetics, poor selectivity compared to enzymatic sensors, and the need for alkaline solutions^{40,41}. Efforts to address these challenges have led to the exploitation of (1) nanostructured electrodes for increased contact area with the bioanalytes, and (2) a porous cavity containing mild alkali solutions for sweat glucose analysis³⁰. Nevertheless, these electrochemical sweat devices in various forms (e.g., wristband More accurate results in²⁹, headband⁴², or skin patch¹⁸) provide real-time and convenient readout^{32,43–45}. However, electronic modules inevitably increase the cost and footprint of the resulting wearable devices and have compliance issues for the elderly⁴⁶.

Different from electrochemical sensors, colorimetric sweat sensors are more compliant, low-cost, and easy to use due to the elimination of electronics (used for data analysis and transmission). Used as color indicators, the chromophore molecules can change their electron state when interacting with target biomarkers to result in the absorption of photons with different wavelengths, visualized as color changes with intensity correlated with the concentration²⁸. The colorimetric assays with dry reagents added to the reaction chamber can detect a series of biomarkers, including metabolites, electrolytes, and micronutrients. For instance, the generated H₂O₂ from glucose oxidation changes colorless o-dianisidine into red-colored oxidized o-dianisidine, which can detect glucose in range from 0.1 to 0.5 mM with a limit of detection (LoD) of 0.03 mM⁴⁷. Similarly, the increase in the lactate concentration from 0 to 30 mM oxidizes 4-aminoantipyrine to change the color from yellow to purple with LoD of 1.58 mM⁴⁸. The chloride ions (Cl⁻) reacts with silver chloranilate to produce a color response from white to purple in proportional to Cl⁻ concentration from 0 to 120 mM with LoD of 10 mM²¹, whereas calcium ions (Ca²⁺, 0–15 mM) reacts with o-cresolphthalein complexone (o-CPC) to yield a violet-colored complex (LoD of 2 mM)⁴⁹. The detection of vitamin C relies on the reduction of ferric ion (Fe³⁺) to ferrous ion (Fe²⁺) during interaction with vitamin C in the range from 0 to 100 μM to generate a compound with a color change to pink (LoD of 2 μM)⁵⁰. Compared with point-of-care sweat analysis, the wearable colorimetric sensors can provide continuous sweat collection

¹School of Materials Science and Engineering, Xiangtan University, Xiangtan, Hunan 411105, China. ²Department of Engineering Science and Mechanics, The Pennsylvania State University, University Park, PA 16802, USA. ✉email: Huanyu.Cheng@psu.edu; onexf@xtu.edu.cn

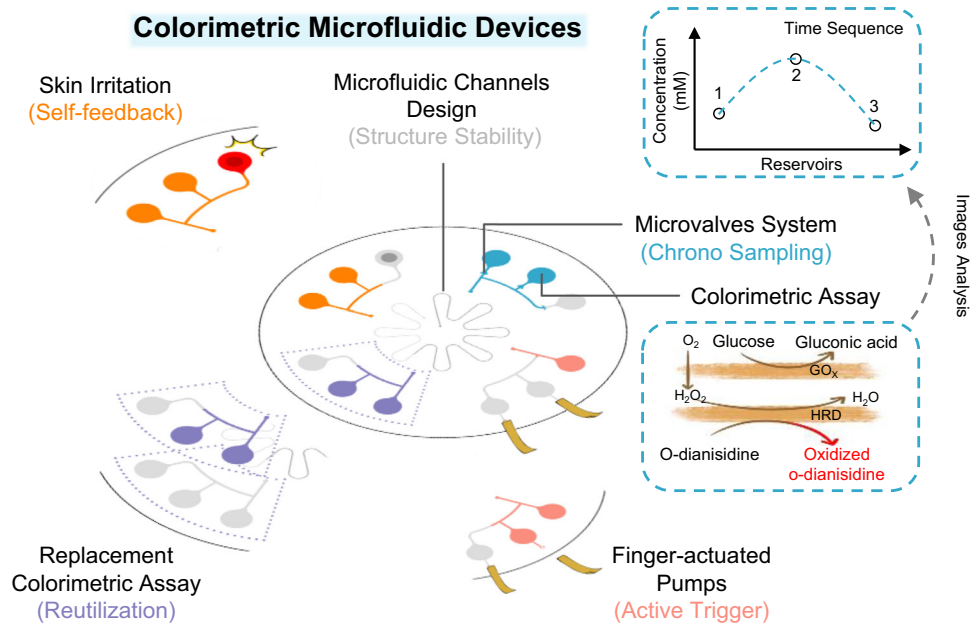


Fig. 1 Schematic diagram of skin-interfaced colorimetric microfluidic devices with colorimetric assay and microfluidic network for sweat analysis and advanced sweat control and feedback.

and analysis over time for early disease diagnostics (e.g., elevated sweat chloride for cystic fibrosis²¹ and increased cortisol levels over prolonged time periods for obesity, depression, hypertension, and diabetes⁵¹). Traditional colorimetric detection relies on the use of a smartphone or the standard colorimetric card for direct comparison because of the difficulty to recognize a single color change with the naked eye⁵². More accurate results in terms of the exact degree of color reaction can be based on a preset coordinate axis in the distance method^{53,54} or multicolor colorimetric methods⁵⁵. However, the most used method is relying on the real-time image analysis of smartphones to provide quantitative readout^{56,57} require the image to be well-framed and uniformly lit^{20,58}. For colorimetric assay measurement, the LAB color space algorithm can be used to accurately extract small differences in color⁵⁹, which enhances reliability in practical scenarios with uncontrolled lighting compared to assessments in the RGB color space⁶⁰. Both traditional computer vision and advanced machine-learning algorithms can also be exploited to assist image capture and feature quantification^{25,58,61,62}. The irreversible color change of the colorimetric sensor is often associated with (1) single or limited-time use, (2) sweat mixing at different time points, and (3) undesired sweat contamination and evaporation to affect sweat analysis⁶³. To address these challenges, the colorimetric sensor is often integrated with microfluidic devices, which also allows the detection of multiple analytes in a single platform²⁰. The microchannel connected with a series of independent storage chambers allows sweat sampling and analysis over time, while minimizing the issues from sweat cross-contamination or evaporation. Although the chromogenic reagent is not reversible to provide “continuous” monitoring^{64,65}, microfluidic networks can be used to separate newly secreted from previous sweat into a series of chambers for temporary storage or sequential detection^{66,67} even in intensive contact sports²⁵ and aquatic settings²⁷. Therefore, the rational design of microfluidic devices makes it possible to reliably monitor the concentration variation of biomarkers in sweat with the colorimetric method.

This review briefly outlines the recent developments of colorimetric microfluidic sweat devices, with an emphasis on chronometric sampling and electronics-free control or feedback technologies (Fig. 1). The former mainly focuses on the structural

design of microfluidic valves, whereas the latter highlights self-feedback reminders and active triggers for closed-loop sweat analysis systems. After reviewing the current limitations, possible directions for future developments are discussed.

Chrono sampling behavior in colorimetric microfluidic sweat devices

In the electrochemical sweat sensors, the circuit module is often used to first electronically program a microfluidic valving system for active biofluid management³² and then generate electrical signals based on the collected biofluids for wireless transmission and visual readouts on a smartphone or electrochromic display^{18,43}.

Without electronic components, the colorimetric sweat sensor can only rely on the natural sweat pressure from osmosis effects to drive sweat through soft microfluidic structures for sweat sampling. Therefore, it is vital to design valve structures in microfluidics to actively manage biofluid flow in microfluidic networks for chrono-sampling and analysis. The commonly used designs include capillary bursting valves^{66–70}, hydrophobic valves⁷¹, and polymer valves⁷².

In the capillary bursting valve (Fig. 2a), the bursting pressure is determined by the microchannel geometry and surface wettability to control the flow of the fluid into different collection chambers⁶⁹ in the programmed order⁶⁷ (Fig. 2b) for offline analysis⁶⁰. For instance, reducing the dimension of a rectangular channel can increase the bursting pressure according to the Young-Laplace equation⁶⁶. Secondly, the bursting valve enables the individual analysis of multiple biomarkers to be performed in the same microfluidic chip⁷³. A series of bursting valves with different burst pressures can also be used to accurately and routinely measure the secretory fluidic pressures generated by eccrine sweat glands at different parts of the body⁶⁶. While the discontinuous flow of sweat may generate bubbles, the bursting valve in each branch of the connected micro-flow channel network can adjust the air pressure in the channel and release the produced bubbles⁶⁹. By modulating the geometry of the microchannel with photolithography, the Tesla valve (Fig. 2c) also accelerates the flow in the forward direction and inhibits the flow in the reverse direction^{74,75}, resulting in one-direction flow (with high diodicity) for fluid

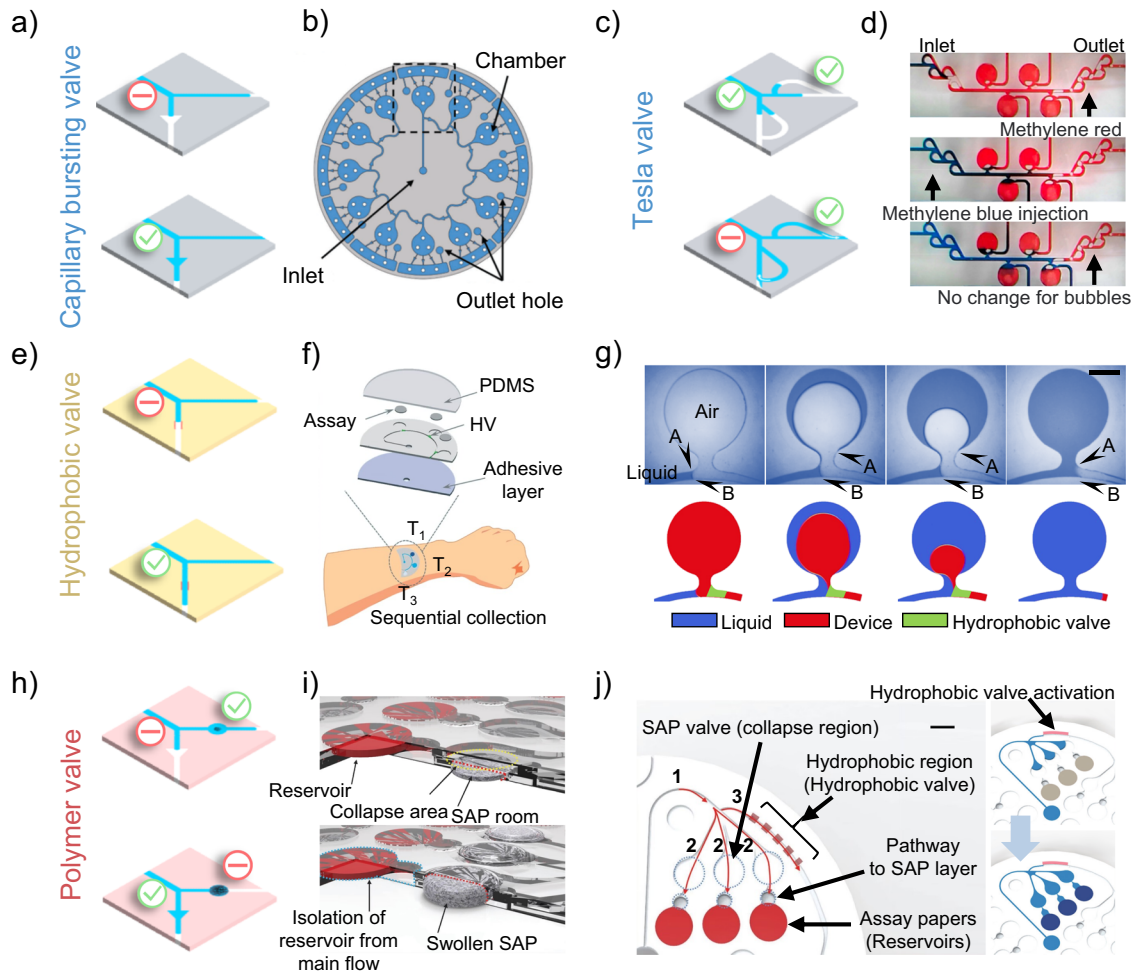


Fig. 2 Skin-interfaced microfluidic chronometric sampling by passive valve structures. **a** Schematic illustration of the capillary bursting valve. **b** Top view of microfluidic channels for chrono-sampling of sweat⁶⁷. **c** Schematic illustration of the Tesla valve and **(d)** its demonstration in the sampling process using methyl red and methylene blue⁷⁴ (increased pressure inside the upper right return channel due to the air pressure). **e** Schematic illustration of the hydrophobic valve (HV) and **(f)** its use in an epidermal microfluidic device with one-opening chambers, along with **(g)** optical images and numerical simulations of the hydrodynamic flow process into the one-opening chamber with a HV⁷¹ (scale bar: 1 mm). **h** Schematic illustration of the polymer valve and **(i)** its use in the super absorbent polymer (SAP) system with valve activation before (top) and after (after) sweat collection⁷². **j** Microfluidic channel design of the combined use of HV and SAP valves with reservoirs⁷² (scale bar: 0.5 mm).

controls. The driving force for the flow in the Tesla valve from the pressure difference between the inlet and outlet⁵⁶ allows the fluid to flow from the high-pressure to low-pressure area (Fig. 2d)⁷⁴. The resulting sweat collection chip prevents backflow at the entrance and restrains the flow to contact the outside at the exit. Without any mechanical structures, the Tesla valve optimizes stability and provides a reusable wearable microfluidic device.

Different from the capillary bursting (Tesla) valve that explores geometric changes of the microchannel, the hydrophobic valve relies on the modulation of the wettability in the inner surface of the microchannel (Fig. 2e). The hydrophobic valve is often prepared by exposing the other (except for valve) regions with plasma to generate hydrophilicity⁷². However, hydrophobic recovery occurs within hours in the ambient environment⁷⁶. Efforts to address this challenge include subsequent surface modification of the plasma-treated PDMS with low-energy polyvinylpyrrolidone (PVP), resulting in long-term stability (6 months)⁷⁷. Introduced at the junction of the chamber and the microfluidic channel, hydrophobic valves can result in the design of one-opening chambers to significantly reduce evaporation and contamination of sweat samples during collection and storage for enhanced accuracy (Fig. 2f)⁷¹. The hydrophobic valve blocks the

advancing front of the liquid so it can spontaneously wick into the hydrophilic chambers, followed by bursting the hydrophobic valve to continue onto the next chamber for sequential collection and chrono-sampling (Fig. 2g). The same mechanism could also be applied to paper-based wearables^{78,79} by embedding the hydrophobic channel barrier (e.g., with wax printing^{62,80}) in the hydrophilic paper microfluidics to direct sweat flow. Because of the capillary flow into the porous paper that causes saturation⁸¹ and its disposable nature, most paper-based microfluidic devices are designed for one-time use only. Combined with a sweat evaporator and pre-defined hydrophobic barriers to drive the continuous sweat flow, the paper-microfluidic devices can allow the flow of fresh sweat across the electrodes and avoid sweat accumulation^{82,83}. However, the durability of paper-based microfluidic devices over long-term use still needs to be thoroughly investigated.

Polymer valves are also simple in design with polymer locally embedded in the microchannel to either expand/contract^{32,72} or dissolve⁸⁴ for reversible or irreversible control of the fluid flow (Fig. 2h). For instance, the polymer valve triggered by a certain amount of collected sweat swells upon hydration to close the inlet passage and prevent backflow while allowing air ventilation

Table 1. Comparison of different microfluidic valves.

| Valve | Capillary bursting valve | Tesla valve | Hydrophobic valve | Polymer valve |
|--------------------|---|---------------------------------|--|--|
| Mechanism | Bursting pressure | Diodicity | Surface wettability | Wettable materials |
| Elements | Microchannel geometry and surface wettability | Difference in flow distribution | Blocking the advancing front of the liquid | Expansion/contraction/dissolution of polymer |
| Types of wearables | Polymer | Polymer | Polymer/ paper/fabric | Polymer/paper |
| Limitations | High precision requirement, long preparation time | | Instability of surface modification | Hysteresis, possible sample contamination |

(Fig. 2i)⁷². The dissolvable polymer valve mainly used in paper-based microfluidics, on the other hand, gradually dissolves itself upon sweat collection to open the valve made entirely of filter paper after a certain time⁸⁴. The other dissolvable barriers made of sucrose^{85,86}, trehalose⁸⁷, or salts⁸⁸ can only slow down the flow (e.g., a delay time of 48 s for the sucrose barrier⁸⁶) without blocking the microfluidic channels, which are suitable for mixing of reagents. The dissolvable polymer valves consisting of dried polymers as a closing valve allow the liquid to flow in sequence to different multisensory transducers for revealing fluctuations in the analyte concentration.

Each type of these valves is associated with advantages and limitations (Table 1) to provide unique application opportunities in chronometric sampling and colorimetric readout. It is also possible to combine different types of valves to leverage the synergy for noninvasive and in situ monitoring of sweat. For instance, the passive polymer valves that route the sweat into the desired reservoirs for analysis and block the channel for preventing backflow after triggering still need to be coupled with other valves (capillary bursting valves or hydrophobic valves) for chronometric sampling. The hydrophobic valves on the primary branches of the microfluidics control the sweat to sequentially close the polymer valves on the secondary branches for stable collection and quantitative analysis (Fig. 2j)⁷².

Electronics-free sweat control or feedback technologies

The major challenges of colorimetric microfluidic devices include (1) uncontrolled flow and mixture of sweat, (2) backflow of soluble chemical reagents from the reaction chamber to the skin, (3) uncertainty in the precise analysis time due to varied sweat rate, (4) difficulty to perform multi-step colorimetric assays, (5) irreversible colorimetric reaction for continuous analysis, and (6) lack of in-time self-feedback. A potential solution to some of the above challenges could explore the combination of the sweat analysis system with an electronically programmable microfluidic valve that uses the individually addressable microheater to control the sweat flow in the microchannels blocked by the thermos-responsive hydrogel³². The active control of the valves allows sweat analysis at user-defined times, independent of sweat flow rate and external disturbances. The electrochemical sweat analysis combined with a wireless flexible printed circuit board (FPCB) also allows reversible sweat analysis and instant feedback. Although a complete solution for electronics-free colorimetric microfluidic devices is yet to be reported, the inspiration from the above electrochemical sweat analysis system and many others could open up opportunities for future developments.

The use of relatively high modulus polymers (e.g., polyurethane resin with a Young's modulus of 1.1 GPa) as relatively rigid but deformable serpentine "skeletal" structures (Fig. 3a)^{89,90} in microfluidics devices can minimize errors caused by microchannel deformation or microcavity collapse⁹¹. The "skeletal" structures are further surrounded by a low-modulus polymer ($E_{\text{substrate},1} = 60$ kPa, $E_{\text{substrate},2} = 1$ MPa) to provide an elastic restoring force and a soft interface to the skin. To prevent the backflow of chemical reagent (and sweat) for reduced risks of potential chemical harm

to the skin, the check valve located between the reaction chamber and microchannels can be explored to direct the sweat flow along the pre-defined direction (Fig. 3b)⁴⁷.

To perform sample analysis at the user-defined time, the finger-actuated pumps are introduced at the end of microchannels (Fig. 3c)⁹². After collecting the pre-defined amount of sweat in the inlet chamber with excess sweat expelled through the outlet, pulling a thin tab can deform the cavity to generate air pressure to suck the collected sweat from the inlet chamber into the sensing chamber for quantitative analysis on-demand. Besides the analysis on-demand, active triggers in microfluidic wearables can also help reset the device that will saturate with sweat over time. The reset feature can also initiate the collection of freshly secreted sweat to avoid mixing with the previously collected sweat for improved accuracy in biomarker analysis. Upon pulling the bottom of the resettable skin-interfaced microfluidic device, sweat from the collection channel would be sucked into the elastomeric suction pump, and then ejected through the outlet once the strain is released (Fig. 3d)⁹³. Acting as a pressure pump, the manually activated reset button can also reset the channel using a negative or positive pressure mechanism (Fig. 3e)⁹⁴. With the reset, expelling the collected sweat from the device once full can provide continuous, prolonged sweat analysis.

The irreversible property of the activated colorimetric assays often renders the colorimetric microfluidic devices to be single-use and disposable. One possible solution to this problem is to replenish the colorimetric assay in a "sweatainer" that is further integrated with an epidermal port interface to provide a long-term and fluid-tight interface with the epidermis (Fig. 3f)⁹⁵. The specific aligned access point on the backside of the epidermal port interface facilitates a rapid replacement of sweatainer within 30 s for a minimized interruption during sweat collection.

The colorimetric microfluidic devices with self-feedback functions to deliver time-sensitive sensations to the skin without electronics can provide critical information such as the physiological status or the device's working status to the users. Therefore, the resulting system can avoid frequent observations and reduce device complexity without using electronics. As a representative example, the sense of touch can provide chemesthesis self-feedback based on an efflux pump that is preloaded with food-grade chemicals (e.g., menthol or capsaicin)⁹³. As the amount of sweat reaches a preset threshold for sweat loss, the released menthol or capsaicin causes skin irritation to actively remind the user of water intake (Fig. 3g). Due to the high sensitivity of human skin to temperature⁹⁶, the thermal warning from endothermic/exothermic chemical reactions triggered by sweat such as the reaction between CaO and water is also promising. However, chemesthesis can contaminate the skin and be erratic (depending on different parts of the body and the sensitivity of different individuals⁹³), whereas thermal warning requires careful control of temperature and duration to prevent burns⁹⁷.

Conclusions and perspectives

Different from the electrochemical sweat sensors, the detection of biomarkers in sweat with colorimetric sweat sensors relies

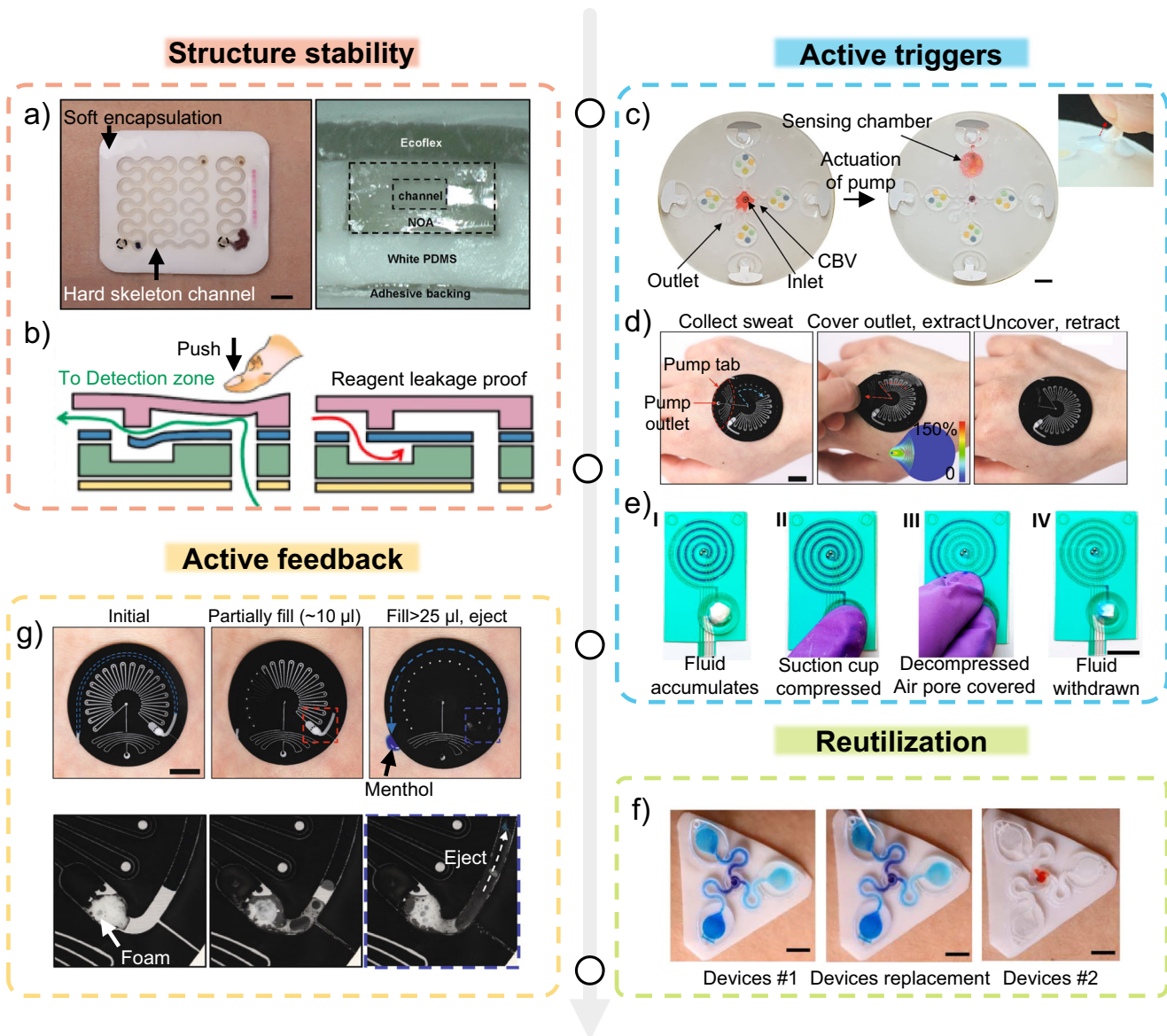


Fig. 3 Electronics-free sweat control and feedback technologies in colorimetric microfluidic devices. Enhanced structure stability with (a) rigid microchannels embedded in a soft elastomer⁸⁹ (scale bar: 5 mm) and (b) check valves in microchannels to prevent reagent backflow⁴⁷. Active trigger with (c) finger-actuated pumps for on-demand sweat analysis⁹² (scale bar: 5 mm), (d) strain-actuated pinch valve for microchannels reset⁹³, and (e) manually activated button for negative pressure suction reset⁹⁴ (scale bar: 1 cm). f Reuse with replenishment of sweat tainer for multiple colorimetric analysis⁹⁵. g Sweat-triggered chemesthetic feedback (C.A. = chemesthetic agent)⁹³.

on the design of valve structures and colorimetric reagents. The design of varying valves with different structures and materials provides opportunities to control sweat flow, chronological collection, and quantitative detection. Combined with advanced sweat control and feedback technologies, the electronic-free colorimetric microfluidic device starts to show the potential for closed-loop devices. Combining colorimetric reagents with different materials such as fabric⁴², paper^{22,98}, and hydrogel^{99,100} facilitates the colorimetric readout (e.g., accurate measurements of sweat rate due to measurable swelling and color change in hydrogels¹⁰⁰). Effectively fixing colorimetric reagents in these well-designed substrate materials also prevents color leaching, chemical diffusion, and spatially nonuniform color responses (caused by the continuous flow of sweat). Despite the significant advances, there are still many grant challenges in the field of colorimetric sweat sensors before they can achieve an improved level of comfort,

stable functions upon mechanical deformation, and reliable manufacturing at a low cost for various applications.

The soft and deformable design of the wearables is needed to reduce discomfort and iatrogenic injury, especially for those with delicate skin such as infants^{101,102}. However, the deformation of the device during operation or other non-specific external factors can affect the sweat flow behavior in microfluidic devices or even accidentally trigger the feedback component. Although the microfluidic devices with relatively rigid microchannels and soft substrate can be explored to alleviate this issue, the fabrication involves expensive and time-consuming processes (photolithography and deep reactive ion etching with encapsulation over 16 h), as well as large material and modulus mismatch^{89,90}. In comparison, the digital light processing (DLP) technology could provide rapid fabrication (<1 h) of 3D printed channels with micron-scale feature sizes (<100 μ m) and enhanced optical transparency (Fig. 4a)⁹⁵. Meanwhile, the grayscale in DLP allows

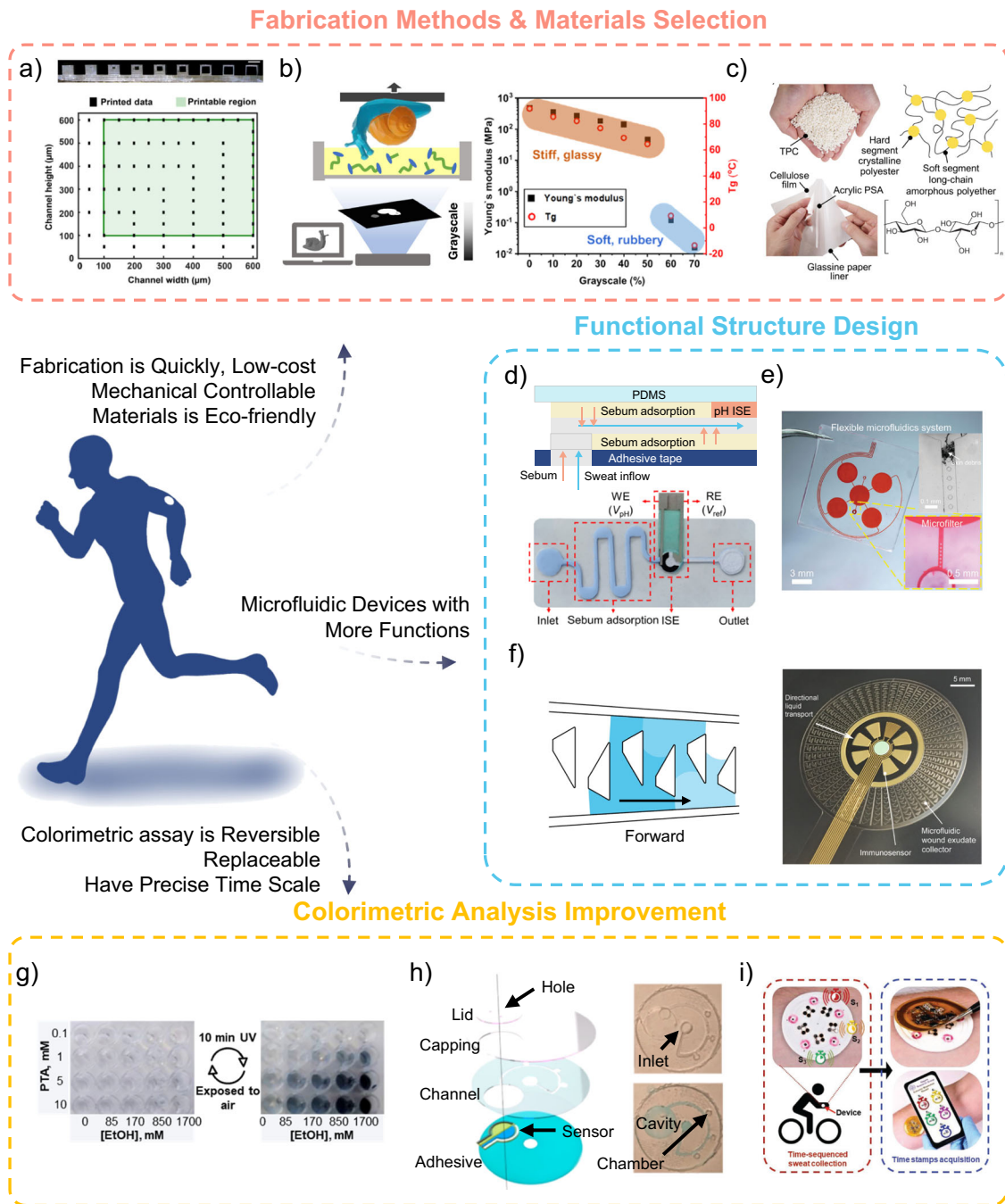


Fig. 4 Future opportunities for wearable colorimetric sweat monitoring systems. The use of digital light processing (a) to fabricate microfluidic devices⁹⁵ and (b) its grayscale to fabricate mechanically gradient materials¹⁰³. c Eco-friendly microfluidic devices consisting of biodegradable thermoplastic copolyester elastomer (TPC) for the microfluidic layer and a cellulose film with an acrylic pressure-sensitive adhesive (PSA) for the sealing layer⁶⁰. d Common oil-control sheets to filter sebum in sweat¹⁰⁵. e Microfluidic devices with ten micropillars in the inlet to filter microspheres and skin debris⁴⁴. f The directional liquid transport system that exploits the interconnected sawtooth-shaped capillary channels with wedge-shaped micropillar array¹⁰⁶. g Color change diagram of PTA/ethanol photo-redox cycle¹⁰⁸. h The exploded view of the integrated microfluidic non-enzymatic glucose sensor with a replaceable porous encapsulating reaction cavity³⁰. i The colorimetric analysis with precise time point to determine the temporal variations of biomarkers in sweat¹⁰⁹.

the use of different intensities of light to fabricate the functionally graded materials with a mechanical gradient up to three orders of magnitude, mitigating the issue of abrupt modulus difference (Fig. 4b)¹⁰³. To mitigate the environmental concerns from disposed devices, the commonly used silicone elastomer such as PDMS and Ecoflex¹⁰⁴ can be replaced by biodegradable materials. For instance, a biodegradable microfluidic device consisting of thermoplastic copolyester elastomers (TPCs) for the microfluidic

layer, a cellulose film and pressure-sensitive adhesive as a sealing layer, and natural chemical reagents as colorimetric assays can be fully degraded in the soil to organic compounds for plant growth (Fig. 4c)⁶⁰.

In addition, accurate sweat analysis with skin-interfaced wearables needs to mitigate the contaminants secreted from the skin (e.g., sebum, skin debris, dust). A paper-based sandwich-structured pH sensor that uses common oil-control sheets can

filter the sebum mixed in sweat (Fig. 4d)¹⁰⁵. With ten micropillars in the inlet for sweat filtration, the integrated microfluidic chip can effectively filter out microspheres with a diameter of 20 μm and skin debris (Fig. 4e)⁴⁴. The micropillars can also be designed into a wedge shape to form a polar array of interconnected sawtooth-shaped capillary channels and allows the continuous flow in the forward (or reverse) direction is facilitated (or inhibited) (Fig. 4f)¹⁰⁶. Moreover, anti-collapse needs to be considered when designing the micropillars to effectively avoid the collapse of arbitrary-shaped soft microchannels or reservoirs¹⁰⁷.

Most of the colorimetric sweat sensors also suffer from a one-time use of the reagents and non-continuous measurements, despite the recent developments in recyclable colorimetric reagents such as phosphotungstic acid (PTA) for alcohol detection in saliva and sweat. As a colorless photochromic heteropoly acid, PTA can be reduced by ethanol to produce an intense blue color under ultraviolet radiation, which can be oxidized and returned to a colorless state after exposure to air (Fig. 4g)¹⁰⁸. Before the advent of reversible colorimetric reagents, the use of replaceable colorimetric devices can be an alternative. The design concept of a replaceable porous encapsulating reaction cavity (Fig. 4h)³⁰ may be leveraged for the robust reagent chamber. It is also of high interest to determine the chamber filling time for obtaining the temporal variation of sweat biomarkers. The colorimetric microfluidic device integrated with sweat-triggered flexible galvanic cells can serve as sweat-activated “stopwatches” to record temporal information associated with the collection of discrete microliter volumes of sweat (Fig. 4i)¹⁰⁹. The galvanic cells triggered by sweat generate a time-dependent decayed voltage that is recorded and obtained with a battery-free NFC module to serve as a “stopwatch”. Although the finger-actuated pumps can provide on-demand sweat analysis, the needed user engagement can be challenging in practical use, so automatic trigger or self-feedback is desirable.

Received: 7 April 2023; Accepted: 15 August 2023;

Published online: 01 September 2023

REFERENCES

- Sempionatto, J. R. et al. Wearable chemical sensors for biomarker discovery in the omics era. *Nat. Rev. Chem.* **6**, 899–915 (2022).
- Ates, H. C. et al. End-to-end design of wearable sensors. *Nat. Rev. Mater.* **7**, 887–907 (2022).
- Ghaffari, R. et al. Recent progress, challenges, and opportunities for wearable biochemical sensors for sweat analysis. *Sens. Actuators B Chem.* **332**, 129447 (2021).
- Ye, S. et al. Recent progress in wearable biosensors: From healthcare monitoring to sports analytics. *Biosensors* **10**, 205 (2020).
- Bandodkar, A. J. et al. Wearable sensors for biochemical sweat analysis. *Annu. Rev. Anal. Chem.* **12**, 1–22 (2019).
- Bariya, M. et al. Wearable sweat sensors. *Nat. Electron.* **1**, 160–171 (2018).
- Dai, B. et al. Flexible wearable devices for intelligent health monitoring. *View* **3**, 20220027 (2022).
- Luo, D. et al. Flexible sweat sensors: From films to textiles. *ACS Sens* **8**, 465–481 (2023).
- Liu, Y. et al. Skin-interfaced superhydrophobic insensible sweat sensors for evaluating body thermoregulation and skin barrier functions. *ACS Nano* **17**, 5588–5599 (2023).
- Fu, R. et al. A tough and self-powered hydrogel for artificial skin. *Chem. Mater.* **31**, 9850–9860 (2019).
- Kashaninejad, N. & Nguyen, N. T. Microfluidic solutions for biofluids handling in on-skin wearable systems. *Lab Chip* **23**, 913–937 (2023).
- Zhao, J. et al. A structured design for highly stretchable electronic skin. *Adv. Mater. Technol.* **4**, 1900492 (2019).
- Garcia-Carmona, L. et al. Pacifier biosensor: Toward noninvasive saliva biomarker monitoring. *Anal. Chem.* **91**, 13883–13891 (2019).
- Xu, J. et al. Wearable eye patch biosensor for noninvasive and simultaneous detection of multiple biomarkers in human Tears. *Anal. Chem.* **94**, 8659–8667 (2022).
- Chen, Y. et al. Skin-like biosensor system via electrochemical channels for noninvasive blood glucose monitoring. *Sci. Adv.* **3**, e1701629 (2017).
- Lin, P. H. et al. Wearable microfluidics for continuous assay. *Annu. Rev. Anal. Chem.* **16**, 6.1–6.23 (2023).
- Nyein, H. Y. Y. et al. A wearable patch for continuous analysis of thermoregulatory sweat at rest. *Nat. Commun.* **12**, 1823 (2021).
- Hojajji, H. et al. An autonomous wearable system for diurnal sweat biomarker data acquisition. *Lab Chip* **20**, 4582–4591 (2020).
- Yang, D. S. et al. Sweat as a diagnostic biofluid. *Science* **379**, 760–761 (2023).
- Choi, J. et al. Soft, skin-integrated multifunctional microfluidic Systems for Accurate Colorimetric Analysis of Sweat Biomarkers and Temperature. *ACS Sens* **4**, 379–388 (2019).
- Ray, T. R. et al. Soft, skin-interfaced sweat stickers for cystic fibrosis diagnosis and management. *Sci. Transl. Med.* **13**, eabd8109 (2021).
- Koh, A. et al. A soft, wearable microfluidic device for the capture, storage, and colorimetric sensing of sweat. *Sci. Transl. Med.* **8**, 366ra165–366ra165 (2016).
- He, W. et al. Integrated textile sensor patch for real-time and multiplex sweat analysis. *Sci. Adv.* **5**, eaax0649 (2019).
- Yang, Y. et al. A laser-engraved wearable sensor for sensitive detection of uric acid and tyrosine in sweat. *Nat. Biotechnol.* **38**, 217–224 (2020).
- Baker, L. B. et al. Skin-interfaced microfluidic system with personalized sweating rate and sweat chloride analytics for sports science applications. *Sci. Adv.* **6**, eabe3929 (2020).
- Zhong, B. et al. Wearable sweat loss measuring devices: From the role of sweat loss to advanced mechanisms and designs. *Adv. Sci.* **9**, e2103257 (2022).
- Reeder, J. T. et al. Waterproof, electronics-enabled, epidermal microfluidic devices for sweat collection, biomarker analysis, and thermography in aquatic settings. *Sci. Adv.* **5**, eaau6356 (2019).
- Saha, T. et al. Access and management of sweat for non-invasive biomarker monitoring: A comprehensive review. *Small* e2206064, 1–17 (2022).
- Gao, W. et al. Fully integrated wearable sensor arrays for multiplexed in situ perspiration analysis. *Nature* **529**, 509–514 (2016).
- Zhu, J. et al. Laser-induced graphene non-enzymatic glucose sensors for on-body measurements. *Biosens. Bioelectron.* **193**, 113606 (2021).
- Bi, Y. et al. Universal fully integrated wearable sensor arrays for the multiple electrolyte and metabolite monitoring in raw sweat, saliva, or urine. *Anal. Chem.* **95**, 6690–6699 (2023).
- Lin, H. et al. A programmable epidermal microfluidic valving system for wearable biofluid management and contextual biomarker analysis. *Nat. Commun.* **11**, 4405 (2020).
- Kim, J. et al. Noninvasive alcohol monitoring using a wearable tattoo-based iontophoretic-biosensing system. *ACS Sens* **1**, 1011–1019 (2016).
- Zaidi, S. A. & Shin, J. H. Recent developments in nanostructure based electrochemical glucose sensors. *Talanta* **149**, 30–42 (2016).
- Dervisevic, M. et al. Silicon micropillar array-based wearable sweat glucose sensor. *ACS Appl. Mater. Interfaces* **14**, 2401–2410 (2022).
- Oh, S. Y. et al. Skin-attachable, stretchable electrochemical sweat sensor for glucose and pH detection. *ACS Appl. Mater. Interfaces* **10**, 13729–13740 (2018).
- Toghiani, K. E. & Compton, R. G. Electrochemical non-enzymatic glucose sensors: A perspective and an evaluation. *Int. J. Electrochem. Sci.* **5**, 1246–1301 (2010).
- Bae, C. W. et al. Stretchable non-enzymatic fuel cell-based sensor patch integrated with thread-embedded microfluidics for self-powered wearable glucose monitoring. *Adv. Mater. Interfaces* **9**, 2200492 (2022).
- Zhu, H. et al. Advances in non-enzymatic glucose sensors based on metal oxides. *J. Mater. Chem. B* **4**, 7333–7349 (2016).
- Cash, K. J. & Clark, H. A. Nanosensors and nanomaterials for monitoring glucose in diabetes. *Trends Mol. Med.* **16**, 584–593 (2010).
- Teymourian, H. et al. Electrochemical glucose sensors in diabetes management: an updated review (2010–2020). *Chem. Soc. Rev.* **49**, 7671–7709 (2020).
- Zhao, Z. et al. A thread/fabric-based band as a flexible and wearable microfluidic device for sweat sensing and monitoring. *Lab Chip* **21**, 916–932 (2021).
- Yin, L. et al. A stretchable epidermal sweat sensing platform with an integrated printed battery and electrochromic display. *Nat. Electron.* **5**, 694–705 (2022).
- Huang, X. et al. Intelligent soft sweat sensors for the simultaneous healthcare monitoring and safety warning. *Adv. Healthc. Mater.* **12**, e2202846 (2023).
- Nyein, H. Y. Y. et al. Regional and correlative sweat analysis using high-throughput microfluidic sensing patches toward decoding sweat. *Sci. Adv.* **5**, eaaw9906 (2019).
- Li, J. et al. Health monitoring through wearable technologies for older adults: Smart wearables acceptance model. *Appl. Ergon.* **75**, 162–169 (2019).
- Xiao, J. et al. Microfluidic chip-based wearable colorimetric sensor for simple and facile detection of sweat glucose. *Anal. Chem.* **91**, 14803–14807 (2019).
- Yue, X. et al. Simple, skin-attachable, and multifunctional colorimetric sweat sensor. *ACS Sens* **7**, 2198–2208 (2022).

49. He, X. et al. Flexible and superwetable bands as a platform toward sweat sampling and sensing. *Anal. Chem.* **91**, 4296–4300 (2019).
50. Kim, J. et al. A skin-interfaced, miniaturized microfluidic analysis and delivery system for colorimetric measurements of nutrients in sweat and supply of vitamins through the skin. *Adv. Sci.* **9**, e2103331 (2022).
51. Xu, Z. et al. A conducting polymer PEDOT:PSS hydrogel based wearable sensor for accurate uric acid detection in human sweat. *Sens. Actuators B Chem.* **348**, 130674 (2021).
52. Xu, S. et al. A morphology-based ultrasensitive multicolor colorimetric assay for detection of blood glucose by enzymatic etching of plasmonic gold nanobipyramids. *Anal. Chim. Acta* **1071**, 53–58 (2019).
53. Phoonsawat, K. et al. A smartphone-assisted hybrid sensor for simultaneous potentiometric and distance-based detection of electrolytes. *Anal. Chim. Acta* **1226**, 340245 (2022).
54. Tao, Y. et al. Microfluidic devices with simplified signal readout. *Sens. Actuators B Chem.* **339**, 129730 (2021).
55. He, S. et al. Cascaded enzymatic reaction-mediated multicolor pixelated quantitative system integrated microfluidic wearable analytical device (McPIQ- μ WAD) for non-invasive and sensitive glucose diagnostics. *Sens. Actuators B Chem.* **369**, 132345 (2022).
56. Bandodkar, A. J. et al. Battery-free, skin-interfaced microfluidic/electronic systems for simultaneous electrochemical, colorimetric, and volumetric analysis of sweat. *Sci. Adv.* **5**, eaav3294 (2019).
57. Ardalan, S. et al. Towards smart personalized perspiration analysis: An IoT-integrated cellulose-based microfluidic wearable patch for smartphone fluorimetric multi-sensing of sweat biomarkers. *Biosens. Bioelectron.* **168**, 112450 (2020).
58. Baker, L. B. et al. Skin-interfaced microfluidic system with machine learning-enabled image processing of sweat biomarkers in remote settings. *Adv. Mater. Technol.* **7**, 2200249 (2022).
59. Ghaffari, R. et al. Soft wearable systems for colorimetric and electrochemical analysis of biofluids. *Adv. Funct. Mater.* **30**, 1907269 (2019).
60. Liu, S. et al. Soft, environmentally degradable microfluidic devices for measurement of sweat rate and total sweat loss and for colorimetric analysis of sweat biomarkers. *EcoMat* **5**, e12270 (2022).
61. Liu, Z. et al. Explainable deep-learning-assisted sweat assessment via a programmable colorimetric chip. *Anal. Chem.* **94**, 15864–15872 (2022).
62. Yüzer, E. et al. Smartphone embedded deep learning approach for highly accurate and automated colorimetric lactate analysis in sweat. *Sens. Actuators B Chem.* **371**, 132489 (2022).
63. Mohan, A. M. V. et al. Recent advances and perspectives in sweat based wearable electrochemical sensors. *TrAC Trends Anal. Chem.* **131**, 116024 (2020).
64. Qiao, L. et al. Advances in sweat wearables: Sample extraction, real-time biosensing, and flexible platforms. *ACS Appl. Mater. Interfaces* **12**, 34337–34361 (2020).
65. Lyu, Q. et al. Soft wearable healthcare materials and devices. *Adv. Healthc. Mater.* **10**, e2100577 (2021).
66. Choi, J. et al. Soft, skin-mounted microfluidic systems for measuring secretory fluidic pressures generated at the surface of the skin by eccrine sweat glands. *Lab Chip* **17**, 2572–2580 (2017).
67. Choi, J. et al. Thin, soft, skin-mounted microfluidic networks with capillary bursting valves for chrono-sampling of sweat. *Adv. Healthc. Mater.* **6**, 1601355 (2017).
68. Wang, X. et al. Surface wettability for skin-interfaced sensors and devices. *Adv. Funct. Mater.* **32**, 2200260 (2022).
69. Shajari, S. et al. MicroSweat: A wearable microfluidic patch for noninvasive and reliable sweat collection enables human stress monitoring. *Adv. Sci.* **10**, e2204171 (2022).
70. Kim, S. B. et al. Soft, skin-interfaced microfluidic systems with integrated enzymatic assays for measuring the concentration of ammonia and ethanol in sweat. *Lab Chip* **20**, 84–92 (2020).
71. Zhang, Y. et al. Skin-interfaced microfluidic devices with one-opening chambers and hydrophobic valves for sweat collection and analysis. *Lab Chip* **20**, 2635–2645 (2020).
72. Kim, S. B. et al. Super-absorbent polymer valves and colorimetric chemistries for time-sequenced discrete sampling and chloride analysis of sweat via skin-mounted soft microfluidics. *Small* **14**, e1703334 (2018).
73. Zhang, H. et al. Wearable microfluidic patch with integrated capillary valves and pumps for sweat management and multiple biomarker analysis. *Biomicrofluidics* **16**, 044104 (2022).
74. Shi, H. et al. Wearable tesla valve-based sweat collection device for sweat colorimetric analysis. *Talanta* **240**, 123208 (2022).
75. Zhao, P. et al. A time sequential microfluid sensor with Tesla-Valve channels. *Nano Res.* <https://doi.org/10.1007/s12274-023-5778-8> (2023).
76. Wolf, M. P. et al. PDMS with designer functionalities—Properties, modifications strategies, and applications. *Prog. Poly. Sci.* **83**, 97–134 (2018).
77. Hemmälä, S. et al. Rapid, simple, and cost-effective treatments to achieve long-term hydrophilic PDMS surfaces. *Appl. Surf. Sci.* **258**, 9864–9875 (2012).
78. Mogera, U. et al. Wearable plasmonic paper-based microfluidics for continuous sweat analysis. *Sci. Adv.* **8**, eabn1736 (2022).
79. Jain, V. et al. A mass-customizable dermal patch with discrete colorimetric indicators for personalized sweat rate quantification. *Microsyst. Nanoeng.* **5**, 29 (2019).
80. Zhang, Z. et al. A versatile, cost-effective, and flexible wearable biosensor for in situ and ex situ sweat analysis, and personalized nutrition assessment. *Lab Chip* **19**, 3448–3460 (2019).
81. Shay, T. et al. Principles of long-term fluids handling in paper-based wearables with capillary-evaporative transport. *Biomicrofluidics* **14**, 034112 (2020).
82. Li, M. et al. A highly integrated sensing paper for wearable electrochemical sweat analysis. *Biosens. Bioelectron.* **174**, 112828 (2021).
83. Cao, Q. et al. Three-dimensional paper-based microfluidic electrochemical integrated devices (3D-PMED) for wearable electrochemical glucose detection. *RSC Adv.* **9**, 5674–5681 (2019).
84. Vaquer, A. et al. Dissolvable polymer valves for sweat chrono-sampling in wearable paper-based analytical devices. *ACS Sens* **7**, 488–494 (2022).
85. Tu, D. et al. Paper microfluidic device with a horizontal motion valve and a localized delay for automatic control of a multistep assay. *Anal. Chem.* **93**, 4497–4505 (2021).
86. Chu, W. et al. Paper-based chemiluminescence immunodevice with temporal controls of reagent transport technique. *Sens. Actuators B Chem.* **250**, 324–332 (2017).
87. Schilling, K. M. et al. Fully enclosed microfluidic paper-based analytical devices. *Anal. Chem.* **84**, 1579–1585 (2012).
88. He, X. et al. Sensitivity enhancement of nucleic acid lateral flow assays through a physical-chemical coupling method: Dissoluble saline barriers. *ACS Sens* **4**, 1691–1700 (2019).
89. Choi, J. et al. Skin-interfaced microfluidic systems that combine hard and soft materials for demanding applications in sweat capture and analysis. *Adv. Healthc. Mater.* **10**, e2000722 (2021).
90. Kim, S. et al. Soft, skin-interfaced microfluidic systems with integrated immunoassays, fluorometric sensors, and impedance measurement capabilities. *Proc. Natl Acad. Sci. USA* **117**, 27906–27915 (2020).
91. Liu, Y. et al. Collapse of arbitrary-shaped soft microfluidics. *Int. J. Solids Struct.* **252**, 111821 (2022).
92. Mishra, N. et al. A soft wearable microfluidic patch with finger-actuated pumps and valves for on-demand, longitudinal, and multianalyte sweat sensing. *ACS Sens* **7**, 3169–3180 (2022).
93. Reeder, J. T. et al. Resettable skin interfaced microfluidic sweat collection devices with chemesthetic hydration feedback. *Nat. Commun.* **10**, 5513 (2019).
94. Bariya, M. et al. Resettable microfluidics for broad-range and prolonged sweat rate sensing. *ACS Sens* **7**, 1156–1164 (2022).
95. Wu, C.-H. et al. Skin-interfaced microfluidic systems with spatially engineered 3D fluidics for sweat capture and analysis. *Sci. Adv.* **9**, eadg4272 (2023).
96. Park, M. et al. Skin-integrated systems for power efficient, programmable thermal sensations across large body areas. *Proc. Natl. Acad. Sci. USA* **120**, e2217828120 (2023).
97. Huang, Y. et al. Integrated sensing and warning multifunctional devices based on the combined mechanical and thermal effect of porous graphene. *ACS Appl. Mater. Interfaces* **12**, 53049–53057 (2020).
98. Zhang, Y. et al. Passive sweat collection and colorimetric analysis of biomarkers relevant to kidney disorders using a soft microfluidic system. *Lab Chip* **19**, 1545–1555 (2019).
99. Wang, L. et al. Flexible, self-healable, adhesive and wearable hydrogel patch for colorimetric sweat detection. *J. Mater. Chem. C* **9**, 14938–14945 (2021).
100. Zhao, F. J. et al. Ultra-simple wearable local sweat volume monitoring patch based on swellable hydrogels. *Lab Chip* **20**, 168–174 (2020).
101. Chung, H. U. et al. Binodal, wireless epidermal electronic systems with in-sensor analytics for neonatal intensive care. *Science* **363**, eaau0780 (2019).
102. Liu, S. et al. Strategies for body-conformable electronics. *Matter* **5**, 1104–1136 (2022).
103. Yue, L. et al. Single-vat single-cure grayscale digital light processing 3D printing of materials with large property difference and high stretchability. *Nat. Commun.* **14**, 1251 (2023).
104. Qi, D. et al. Stretchable electronics based on PDMS substrates. *Adv. Mater.* **33**, e2003155 (2021).
105. Yang, M. et al. Paper-based sandwich-structured wearable sensor with sebum filtering for continuous detection of sweat pH. *ACS Sens* **8**, 176–186 (2023).
106. Gao, Y. et al. A flexible multiplexed immunosensor for point-of-care in situ wound monitoring. *Sci. Adv.* **7**, eabg9614 (2021).

107. Wang, X. et al. Anti-self-collapse design of reservoir in flexible epidermal microfluidic device via pillar supporting. *Appl. Phys. Lett.* **113**, 163702 (2018).
108. Sánchez, M. et al. Photochromic polyoxometalate-based enzyme-free reusable sensors for real-time colorimetric detection of alcohol in sweat and saliva. *Mater. Today Chem.* **21**, 100491 (2021).
109. Bandodkar, A. J. et al. Soft, skin-interfaced microfluidic systems with passive galvanic stopwatches for precise chronometric sampling of sweat. *Adv. Mater.* **31**, e1902109 (2019).

ACKNOWLEDGEMENTS

This research was supported by the National Natural Science Foundation of China (12172319 and 11872326), Natural Science Foundation of Hunan Province (2021JJ30648 and 2021JJ30641), Scientific Research Fund (22A0130) of Hunan Provincial Education Department, Furong Scholars Programme of Hunan Province, "Chunhui Program" Cooperative Research Fund (HZKY20220357) of the Ministry of Education, and Postgraduate Scientific Research Innovation Project of Hunan Province (CX20230658). H.C. also acknowledges the support from the National Institutes of Health (Award Nos. R21EB030140, R21OH012220, and R61HL154215), the National Science Foundation (NSF) (Grant Nos. ECCS-2222654 and 1933072), and Penn State University.

AUTHOR CONTRIBUTIONS

W.Y.L., H.Y.C. and X.F.W. conceptualized the work. W.Y.L. wrote the original draft; H.Y.C. and X.F.W. reviewed and edited the manuscript. H.Y.C. and X.F.W. provided overall supervision of the work.

COMPETING INTERESTS

The authors declare no competing interests.

ADDITIONAL INFORMATION

Correspondence and requests for materials should be addressed to Huanyu Cheng or Xiufeng Wang.

Reprints and permission information is available at <http://www.nature.com/reprints>

Publisher's note Springer Nature remains neutral with regard to jurisdictional claims in published maps and institutional affiliations.



Open Access This article is licensed under a Creative Commons Attribution 4.0 International License, which permits use, sharing, adaptation, distribution and reproduction in any medium or format, as long as you give appropriate credit to the original author(s) and the source, provide a link to the Creative Commons license, and indicate if changes were made. The images or other third party material in this article are included in the article's Creative Commons license, unless indicated otherwise in a credit line to the material. If material is not included in the article's Creative Commons license and your intended use is not permitted by statutory regulation or exceeds the permitted use, you will need to obtain permission directly from the copyright holder. To view a copy of this license, visit <http://creativecommons.org/licenses/by/4.0/>.

© The Author(s) 2023